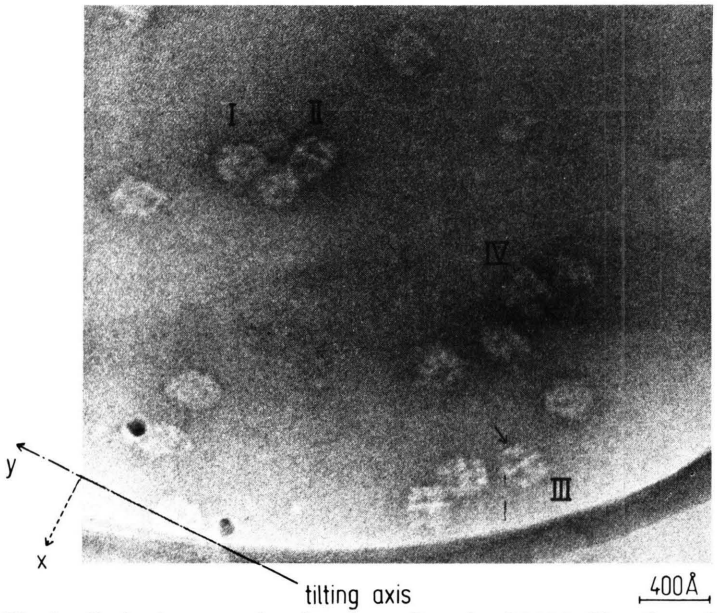

Fig. 2 a. Projection example taken from tilt series S 168-1. The tilt angle was $-40°$. The tilt axis determined à posteriori is in the lower left corner.

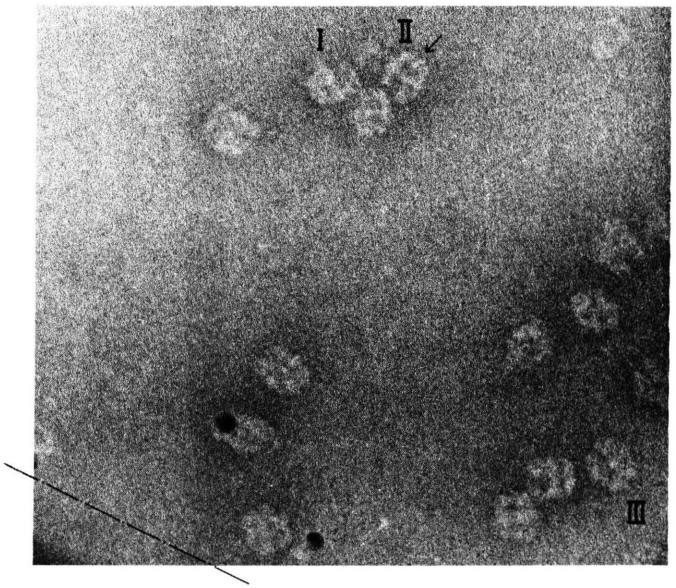

Fig. 2 b. Same object as in Fig. 2 a, tilt angle $-10°$.

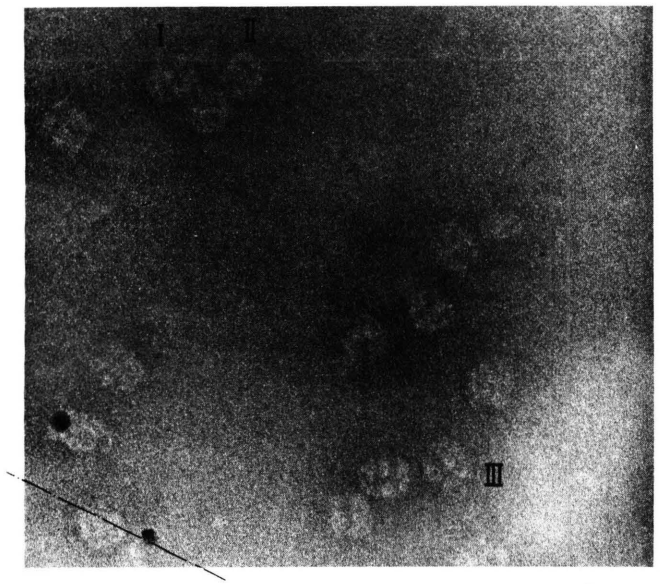

Fig. 2 c. Same object as in Fig. 2 a, tilt angle $+10°$.

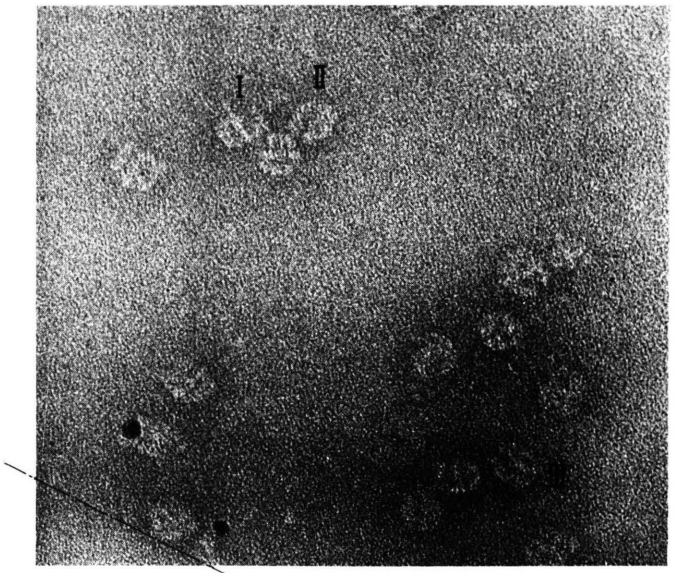

Fig. 2 d. Same object as in Fig. 2 a, tilt angle $+30°$.

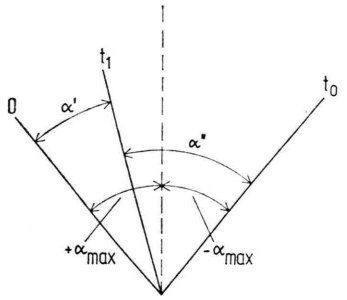

Fig. 16. One cycle reconstruction of radiation damaged features.

work. The tilting angles increase with t. A local feature disappearing at t_1 will only be imaged within a tilting angle range of α'. Its three-dimensional image will be reduced in weight, but it will appear in the correct position. However, due to the restricted tilting angle range it will be distorted with increased clutter. A feature appearing at t_1 will be imaged during α'' showing again a reduced weight and an increased distortion. The important point is that in the one-cycle scheme a correct averaging will also take place although with increased distortions and clutter in the averaged images of the unstable structural features.

Conclusions

It is evident that the restrictions in the present experimental technique lead to pronounced artefacts in the reconstructions. The most serious artefacts stem from the limited angular tilt range, leading to low resolutions in the z-direction and "oversharpening" in the x-direction. However, the test calculations on a structure resembling a real structure (imaged at non-atomic resolutions) have shown that with some care one can recognize the main features of the structure. Compared to this, the test calculations prove that the other artefacts (produced by the restricted tilt interval and by the ill-defined three-dimensional body) are of minor importance. The basic image resolution of the Cormack-Smith reconstruction, is a factor of ~ 2 better than the marginal resolution (1). No amplification of noise will be found under these conditions. The determination of the common tilt axis by correlation of inclined projections has been successfully tested in the various reconstructions.

A comparison of the one-cycle scheme with quasi-simultaneous reconstruction shows that only the latter scheme gives a correctly averaged image of the stable and the unstable structure. The one-cycle scheme averages correctly over the stable structure, but reproduces a cluttered and distorted average over the unstable structural features.

It is encouraging that the main artefacts can be substantially reduced by development of the experimental techniques (increase of the number of projections, conical tilting, see also part I).

Supported by the Deutsche Forschungsgemeinschaft (the biological work especially by the Sonderforschungsbereich 51, Medizinische Molekularbiologie und Biochemie in München) and the Fonds der Chemischen Industrie. We should like to express our sincere thanks.

[1] W. Hoppe, Z. Naturforsch. **30a**, 1188 [1975].
[2] It should be mentioned that the position of markers in electron microscopy is obscured by the structure of the support (see part I).
[3] The cut-off in y-direction is unnecessary, it has only been chosen for ease of computation (square image field).
[4] W. Hoppe, Optik **29**, 617 [1969].
[5] R. A. Crowther, D. J. DeRosier, and A. Klug, Proc. Roy. Soc. London **A317**, 319 [1970].
[6] In Figs. 8 and 9 of part I the size of the reconstruction range ($2R = 300$ Å) has erroneously been omitted.
[7] N. Hunsmann, Doctoral Thesis, Technische Universität München 1975.
[8] H. Rose, Proc. Eighth Intern. Congr. on Electr. Micr., Canberra, Vol. I, p. 212–213 [1974], Fig. 2 for $\Theta_c/\vartheta_0 = 0$.
[9] Additional difficulties for the solution of the corresponding linear equations will be induced by the approximate periodicity of the $\sin x/x$-function with increasing x.
[10] W. Hoppe, P. Bußler, A. Feltynowski, N. Hunsmann, and A. Hirt, Image Processing and Computer-aided Design in Electron Optics, Ed. P. W. Hawkes, Acad. Press, London and New York 1973, p. 92–126. — R. Hegerl and W. Hoppe, Z. Naturforsch., in print.
[11] R. A. Crowther, L. A. Amos, and A. Klug, Proc. Fifth Congr. on Electr. Micr., Manchester 1972, p. 593–597.
[12] A. Klug and R. A. Crowther, Nature London **238**, 435 [1972].
[13] R. A. Crowther, Proc. Eighth Intern. Congr. on Electr. Micr., Canberra 1974, Vol. I, p. 312–313.
[14] R. Hegerl and W. Hoppe, Nature, in preparation.

Three-Dimensional Electron Microscopy of Individual Biological Objects

Part III. Experimental Results on Yeast Fatty Acid Synthetase

W. Hoppe, H. J. Schramm, M. Sturm, N. Hunsmann *, and J. Gaßmann

Max-Planck-Institut für Biochemie, Abteilung für Strukturforschung I, Martinsried bei München, West Germany

(Z. Naturforsch. **31 a**, 1380–1390 [1976]; received September 6, 1976)

Experimental results of three-dimensional reconstructions of individual fatty acid synthetase (FAS) molecules are reported. The discussion of the structures has been concentrated on the symmetry relations within the molecules. A molecular structure with 6 copies arranged in point group 32 is probable. The limits of minimal radiation dose reconstruction are estimated.

Introduction

Experimental work on negatively stained fatty acid synthetase molecules (abbreviated FAS in the following) will be reported. The tilting series have been photographed with overall doses of several C/cm^2. It is obviously of great importance to consider the influence of radiation damage of negatively stained specimens. As first demonstrated on TMV, there is an "initial period" with rapid structural changes (dose $\lesssim 0.1$ C/cm^2), followed by a more stable period with relatively little changes up to very high doses [1]. Our experiments have been done within the second stable period. The influence of the damage has been tested by a series of exposures of FAS under identical conditions and without tilting [2]. It has been shown that the damage in this second period can be approximately described as a random walk process with an increasing radiation damage noise with signal to noise ratios, which are significant up to overall doses of several C/cm^2. Thus the doses used in this work are reasonable. However, it should be kept in mind that one is studying a specimen which is already distorted by the initial radiation damage.

With respect to the information content let us recall that even at a limited "biological resolution" of ~ 20 Å (characteristic for negative stained specimens) the overall amount of three-dimensional information contained in the structure of a biogenic macromolecule with a diameter of ~ 300 Å, is of the same order as in a protein molecule of 30 Å diameter at 2 Å resolution! However, the irregularities in filling all cavities in the molecule (FAS has an open structure with large cavities) with the heavy atom salt together with the radiation damage in the initial period cause inconsistencies, which can only be removed by the comparison of several molecules.

It was possible to derive the gross features of the FAS structure from the reconstructions of several molecules (resembling a hollow ellipsoid with a central thin wall perpendicular to the long axis of the molecule). These results have been presented in the 8th Inter. Conf. on Electron Microscopy at Canberra (1974) [3] and also reported in a short communication [4]. However, in this paper the results of three-dimensional reconstruction of FAS molecules will be discussed in more detail, mainly as an example of how to extract information from the reconstructions. Further results on structural details of FAS will be reported elsewhere.

Yeast Fatty Acid Synthetase, Materials and Methods

Fatty acid synthetase is a molecular complex with a molecular weight of 2.3×10^6 Daltons, incorporating 8 different functional procedures. It catalyses the successive steps of fatty acid synthesis [5]. From determinations of coenzymes and molecular weight measurements it is known that fatty acid synthetase consists of 5 or 6 identical subunits. Each subunit itself is composed of 2 peptide chains (A-chain and B-chain) which carry three and five functions respectively [6]. Our material stems from preparations by Lynen and collaborators [7]. We have used for our experiments either the solution received in the last

Reprint requests to Prof. Dr. W. Hoppe, Max-Planck-Institut für Biochemie, Abteilung für Strukturforschung I, *D-8033 Martinsried bei München.*

* Present address of Dr. Hunsmann, Bayer AG, D-5090 Leverkusen.

preparation step (0.1 M potassium phosphate buffer at p_H 6.5) or a solution of an ammonium sulphate precipitate (90% saturation, stored at −15 °C) in the same buffer (desalted by Sephadex G-25 chromatography or an ultracentrifuge run at 100 000 g for 6 hours). The specific activities were 1500 to 2000 m-units/mg (depletion of malonyl − CoA).

Cross-linking

In some experiments cross-linking has been performed with glutaraldehyde or with dimethyl 3.3-(tetramethylenedioxy)-dipropionimidate dihydrochloride [8]. Cross-linking had no visibly detectable influence on the results.

Grids

Holey collodium films were strengthened with a strong carbon layer and the films overlaid with a thin 50 Å carbon film floated from a mica sheet. The grids were tempered at 180 °C for one hour. Some of the grids were also sparsely coated with gold particles, evaporated onto the thick carbon film. Al_2O_3 films have also been used [9].

Staining

The protein solution of approximately 1 mg/ml, obtained as above, was diluted 1:1 with a freshly prepared 2% PTA solution at p_H 7.4 containing 0.4% glucose. The mixture was sprayed onto the carbon grids using a medical spray.

Electron Microscopy

The electron micrographs were taken with a Siemens Elmiskop 101 or 102 at 100 kV. The microscope was equipped with a lift stage and a microgoniometer (see part I). Translational shift corrections and focusing was done on specimen regions different from the exposure regions, as described in part I. The microscopes were equipped with the standard anticontamination trap and a liquid nitrogen trap [10] in the vacuum chamber which contains the photographic plates. In some experiments it was advantageous to reduce contamination by etching with oxygen entering the microscope near the sample.

The photographic plates (Kodak Electron Image Plates or Agfa Gevaert Sciencia 23 D 50) were developed at constant temperature with nitrogen stirring (Metinol Agfa Gevaert, 10 min; Superfix Tetenal, 10 min).

Densitometry

A flat table densitometer with magnetic tape output (developed in our laboratory) has been used.

Micrographs

Most of the conventional electron microscope images show elliptical figures, which are divided into two apparently equal parts by a central bar. Figure 1* shows a micrograph with negatively stained FAS molecules (taken from one of the series studied in [2]). Small angle X-ray diffraction [11] indicates a hollow rotational ellipsoid. By assuming a central wall perpendicular to the long axis (suspected from the micrographs) improved the agreement with the X-ray scattering curve.

Table 1 shows the tilting series which were used for three-dimensional reconstruction. Some of the reconstruction results have been reported earlier, e. g. molecule S 166-3-II in [3], molecule S 168-1-III in [4]. The reconstructions showed a hollow ellipsoid with a planar central density, proving that the model in [11] is essentially correct. Series S 184-2 together with other unreported series have been taken for the purpose of testing reconstruction under more stringent minimal dose conditions. Therefore, these series were taken with a relatively low electron optical magnification and resolution.

Figure 2 a – d shows four projections of the nine tilted projections taken from series S 168-1. The different focusing in the single projections requires two-dimensional image reconstructions. Figure 3 a – c shows light diffractograms of the projections at −10° (Fig. 2 b), +20° (not shown in Fig. 2), and +30° (Figure 2 d).

After the selection of the molecules to be reconstructed (e. g. S 168-1-I to S 168-1-III in Fig. 2) the

Table I. Data of molecules selected for three-dimensional reconstruction.

Series	Number of reconstructed molecules	Tilting range (number of projections)	Angular increment	Integral radiation loading	Electron optical magnification	Approximate resolution in the micrographs
S 166-3	3	+40° −40° (9)	10°	several C/cm²	120 000	8 Å
S 168-1	3	+40° −40° (9)	10°		154 000	6 Å
S 184-2	2	+50° −46° (9)	12°	0.7 C/cm²	60 000	20 Å

* Figures 1, 2 a–d, 3 a–c, 16 on page 1382 a–b.

corresponding regions have been measured in the densitometer, reconstructed in two dimensions and correlated for a common tilt axis. The final three-dimensional reconstructions have been plotted in sections perpendicular or parallel to the tilt axis. The diameter of the reconstructed cyclinder in most cases was 330 Å (in some cases larger reconstruction volumes have been chosen). For a tilting range up to $\alpha_{max} \sim \pm 40^\circ$ and $\Delta\alpha = 10^\circ$ image point shapes of Fig. 9, part I will occur. The crystallographic resolutions of the reconstructions discussed in detail in this paper (S-168-I) are approximately 30 Å in x-direction, and 45 Å in z-direction. The resolution in y-direction corresponds to the projection resolution ($\sim 6-10$ Å).

Some General Considerations Concerning the Symmetry of the FAS Structure

The first problem in this respect is the separation of the molecules into two substructures divided by the central wall. According to the found hollow ellipsoid and central wall structure, the $5-6$ identical subunits which build up a molecule must have a sheet-like or net-like general structure. However, for a discussion of the symmetry a schematic representation of the subunits by curved bars ("wires") is more convenient. A construction of a body with twofold symmetry and with an odd number of subunits requires special structural features in the subunits. Figure 4 c shows an approximate separation into two parts obtained with 5 subunits, by assuming that the subunits contain pseudo-symmetry elements (schematically sketched in Figure 4 b). The molecule has the point group symmetry 5 (Figure 4 a). The subunit must contain a twofold axis (or pseudo-

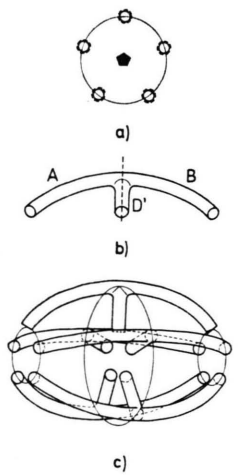

Fig. 4. Symmetry considerations demonstrated on a wire model. For a complex composed of an odd number of subunits a possible division into two equal parts implies a twofold symmetry of the individual subunit.

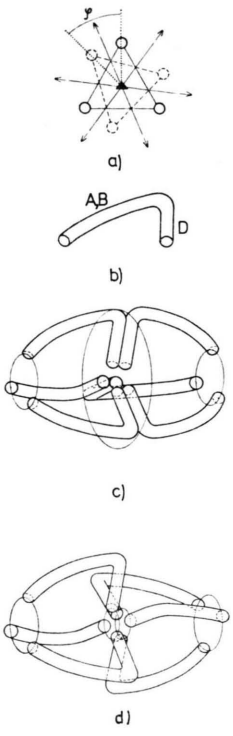

Fig. 5. Symmetry considerations for a complex composed of an even number of subunits. In this case a formation from asymmetric subunits is possible leaving several possibilities for the spatial arrangement.

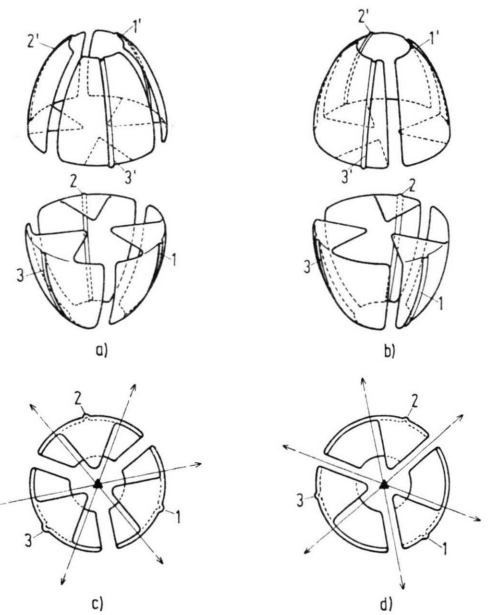

Fig. 6. Schematic diagram to indicate that properly formed subunits can be arranged to build a hollow ellipsoid with a central wall. The shape of the subunit is not determined by symmetry alone, see different boundaries with respect to the stripes 1, 2, 3 and 1′, 2′, 3′ respectively in Fig. 6 a, c, 6 b, d (1, 2, 3 and 1′, 2′, 3′ in same positions with regard to the symmetry elements). For clarity the two halves of the molecule in Fig. 6 a, b have been separately drawn. Figure 6 c, d show only the lower halves of Figure 6 a, b.

axis, pseudo-mirror plane), if a 5-membered structure with twofold symmetry (Fig. 4 a and 4 c) is to be established. However, if we assume 6 subunits, a structure with the point group symmetry 32 can be constructed from asymmetric copies, showing the desired separation (Figure 5). In point group 32 a threefold axis and 3 twofold axes must occur (Figure 5 a). The relative orientation φ in Fig. 5 a is not determined by symmetry. Figure 5 c and Fig. 5 d show two "wire structures" with $\varphi = 0$ and $\varphi = 60°$, composed of the subunits in Figure 5 b. Note, that Fig. 4 b and Fig. 5 b do not represent real models. In the real case using sheets instead of bars, φ can only be defined with respect to a certain structural element in the subunit. Figure 6 only schematically demonstrates that 6 subunits in the shapes of appropriately bent sheets could be combined to form a hollow ellipsoid with a central wall.

Discussion of the Micrographs

The analysis of the three-dimensional reconstruction will later show that only in very rare cases is the long axis of the molecular complex oriented parallel to the supporting foil. For example in Fig. 2 the long axis of molecule III is inclined by $\sim 15°$ to the foil plane. Due to the relative orientation between tilting axis and molecular axis only in Fig. 2 a ($-40°$ tilt) is the central wall parallel to the projection direction and will be imaged as a sharp line. The separation of molecule III into two parts appears quite distinctly in Figure 2 a. However, inspection of the micrographs shows that the heavy atom staining is not completely uniform. The lower right part of molecule III is less stained than the upper left part (see arrow).

Molecule II is inclined by 39° to the supporting foil. This inclination causes a diffuse image of the central wall in Figure 2 b. Figure 2 a (inclination angle $-40°$) shows the central wall as a sharp line. Also in this case the preparation artefacts can easily be seen: In the lower left part of the molecule (see Fig. 2 b) a stronger stain deposition is present, even more pronounced in Figure 2 a. Note for molecule IV, the halves are unequal due to additional artefacts (Figure 2 a). It is obvious that these artefacts must show up in the reconstructions. They will appear even more pronounced, as no averaging by projection takes place. Deducing significant details in a three-dimensional reconstruction must be done with great care even if the projections appear to be quite good.

The orientation of the coordinate system for reconstruction calculations is established in Figure 2 a. For a tilt angle of 0° the supporting foil lies in the x, y-plane (y-direction is the tilt axis) and z-axis points downwards. The molecules are fixed on the lower side of the support. In the case of a positive tilting angle the specimen regions with positive x move upwards.

We now discuss the three-dimensional reconstructions. The reconstruction range is a cylinder with a diameter of 330 Å and a height of 330 Å. For the representation of the results this cyclinder was divided into 64 sections parallel or perpendicular to the cyclinder axis (= calculated tilt axis). The spacing between the sections is therefore ~ 5 Å.

Twofold Symmetry in the Molecule S 168-1-II

The molecule S 168-1-II has a special orientation: Its long axis is perpendicular to the tilt axis. Figure 7 a and b show an x-, z-section through the center of the reconstruction space with positive and negative contour lines respectively. Figure 7 b images the distribution of the negative stain. If we assume that the stain penetrates into all cavities, protein regions with microcavities (non-resolved in the image) will become only partially stained, whereas regions densely packed with protein remain entirely unstained (low density in the image function). Thus Fig. 7 a can be understood as a representation of the protein distribution. In Fig. 7 b the zero line corresponds to the averaged density. The discrimination between "stain" and "protein" by this zero line is arbitrary. It is obvious that this interpretation depends on the smooth occupation of the space either by stain or by protein. Cavities not filled by stain will appear as dense regions in Fig. 7 a, and can be misinterpreted as destroyed protein. A similar error occurs, if nonstained regions of organic material with different density occur. Their contrast difference will be inverted. For our reconstructions (series S 166-3 and S 168-1) a volume has been chosen which just circumscribes the molecule. Figure 7 demonstrates in an illustrative way the extra information due to real three-dimensional imaging. The corresponding two-dimensional representation results if one spreads each image detail along the z-axis. Figure 8 a and Fig. 8 b represent a super-

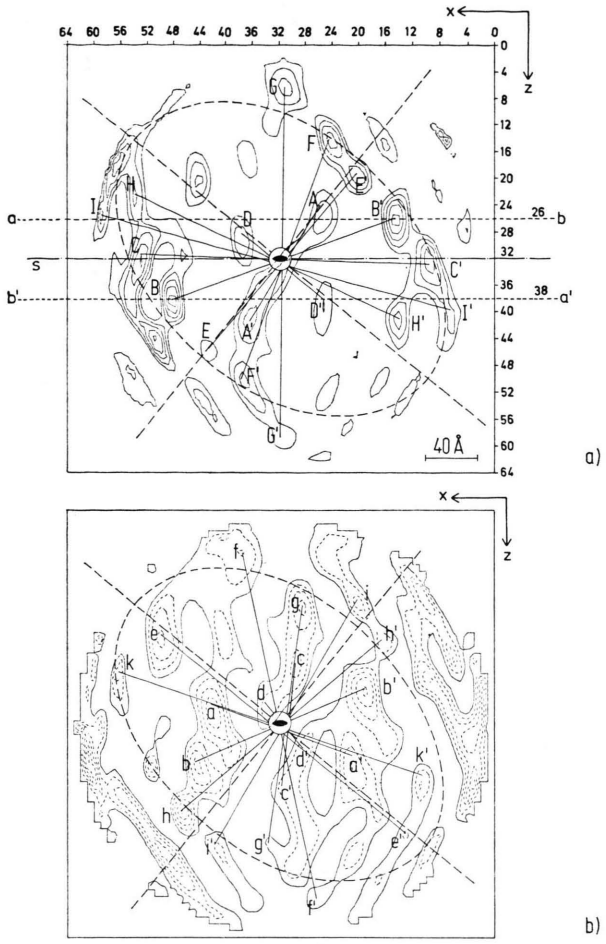

Fig. 7. Twofold symmetry in the density distribution of FAS-molecule S 168-$_1$-II demonstrated on the central section $z=32$, perpendicular to the twofold symmetry axis. The molecular density as well as the stain density show this symmetry quite distinctly, corresponding maxima are connected.

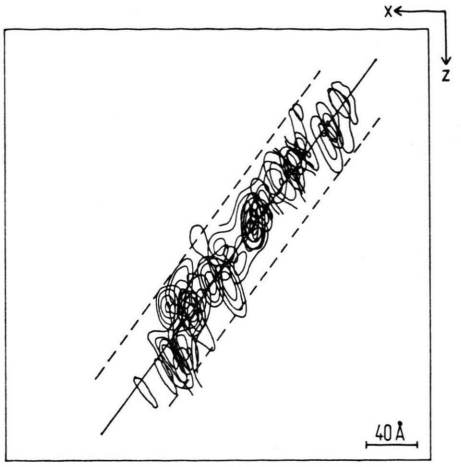

section 18 - 32

Fig. 8 a,

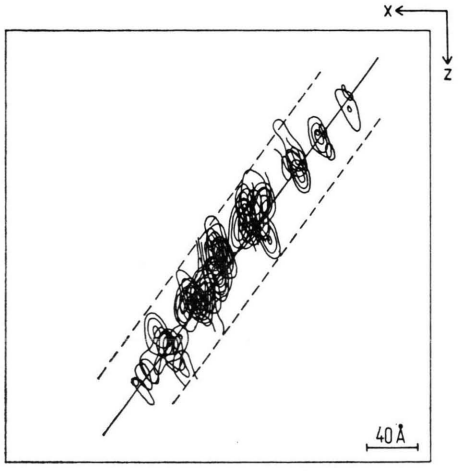

section 32-46

Fig. 8 b.

Fig. 8 a, b. Superposition of densities from the central sections of molecule S 168-1-II to prove the spatial arrangement of the twofold axis parallel to the central wall density. Every second section drawn (total number 64, a) 18–32, b) 32–46).

position along the y-axis of sections 18 – 32 and 32 – 46 respectively in the region of the central wall, thus proving that the tilt axis is indeed parallel to the wall in this case. The wall is planar to a surprisingly good approximation. This image shows for the first time the effect of staining with respect to the third coordinate. No obvious flattening occurs in spite of the large cavities within the molecules.

From Fig. 8 the orientation of the central wall to the support can be determined as 50°. A close inspection of Fig. 7 reveals a relatively well-pronounced twofold symmetry in the structural details. Related maxima (A – I and A′ – I′ respectively) are marked in Figure 7 a. The corresponding heavy atom stain distribution in Fig. 7 b also shows symmetry related maxima. In Fig. 7 a it can be observed that the maxima in the wall (B, C, F, G) and the symmetrically related maxima B′, C′, F′, G′ are quite strong, whereas other surface regions on top and bottom of the figure are weak. In the case of a twofold axis the symmetry must occur in all x, z-sections. By inspection of further sections this symmetry – although not always equally pronounced – has been proven. It is obvious that this twofold axis should also show up in the corresponding x, y-sec-

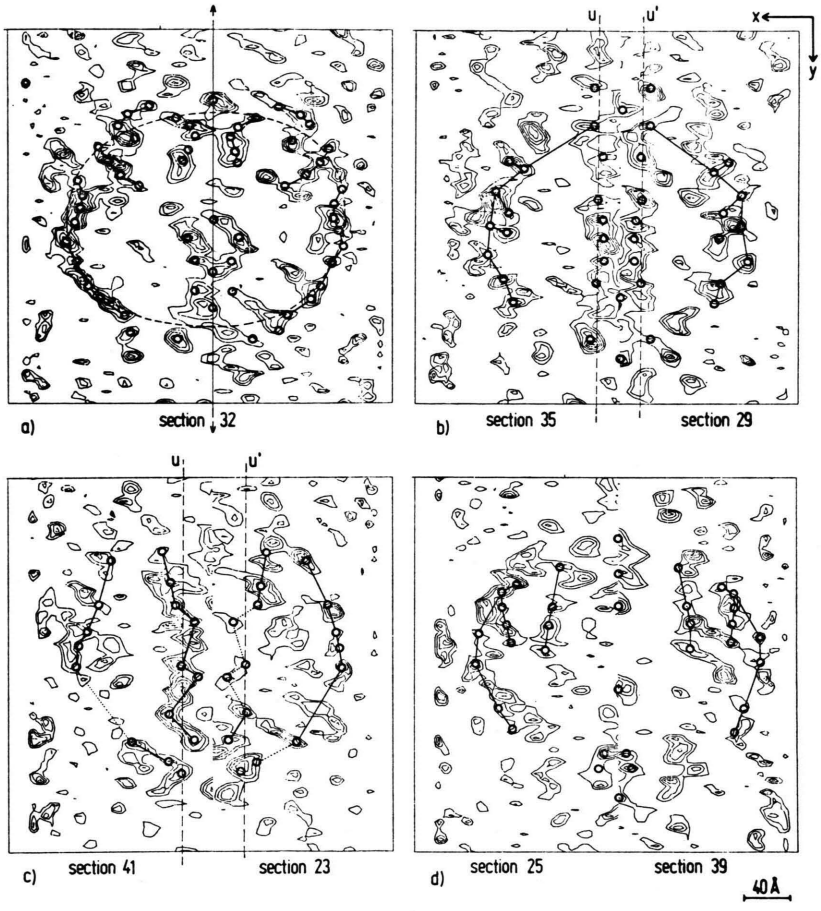

Fig. 9. Comparison of symmetry related sections to further prove the twofold symmetry in the whole three-dimensional density. Respective regions of section $z=32+3$ must coincide with appropriate regions of section $z=32-3$, u, u' = approximate section lines through the wall.

tions. Figure 7 a demonstrates that sections equally distant from the central section $z=32$ should be compared (a and a′, and b and b′ respectively, shown for the section $z=26$ and $z=38$). Let us first regard the central x-y section $z=32$ in Figure 9 a. As Fig. 7 demonstrates, the section should show a nearly circular section through the wall of the ellipsoid and a section through the central wall (appearing as the strongest line). The twofold axis lies in this plane, however, shifted from the center to the right by about 5 Å (see also Figure 8). If the symmetry was exact, the right hand image would be separated from the left hand image by a mirror line. The overall wall shape (nearly circular in this section) and the characteristic fine structure of the walls is immediately apparent. Note the higher resolution in the x, y-plane compared with Figure 7. The symmetric peaks are labelled by black circles. Connecting lines between the circles are drawn in order to facilitate the inspection. Further information about this symmetry is shown by the composite section parts z, z' (see a, a′ in Fig. 7 a). Figure 9 b shows a z, z'-section ($z=35$, $z'=29$) with a distance of ± 15 Å from the central section. As expected, the structure is similar to the structure in Figure 9 a. Due to the low resolution in the z-direction, many features of Fig. 9 a are retained in Figure 9 b. Of special interest is the z, z'-section in Fig. 9 c ($z=41$, $z'=23$), which demonstrates an unequal staining in the wall. The connecting lines in overstained regions are dashed. The sections studied are 90 Å apart. Note that the external wall is also unequally stained. Structural details seem to be "buried" in the stain. This could mean that the protein components in this region are completely destroyed by preparation or radiation. The complement of a z, z'-section is shown in Fig. 9 d ($z=25$, $z'=39$). In the x, y-sections the image of the central wall should appear as straight bars shifted from the right to left with increasing z. Theoretically it should appear in each

x, y-section as a straight bar. However, the breadth of the bar (in the z, z'-sections a double bar) varies appreciably retaining the overall twofold symmetry. But it would be incorrect, to explain these variations as thickness variation of the central wall. We should remember that an x, y-section resembles a partial projection due to the length of the image point in the direction of the z-axis. Thus a certain lateral region of the wall (which will depend on the inclination angle, see Fig. 7) will be projected. It is also evident that the structures of the outer wall in the sections in Fig. 9 are generated by partial projections.

We do not discuss the structure of the individual molecule in further detail. With diagrams combining more distant sections, the symmetry in general becomes weaker, because the central wall tends to stabilize the structures in its immediate neighbourhood. Twofold symmetries have also been found in other molecules – e. g. in S 168-1-III. However, they are there not so easily recognizable as in molecule S 168-1-II, which has a twofold axis oriented along the tilting axis.

It is required that all symmetry searches must be done with great caution. Sometimes quite pronounced accidental symmetries can occur. It is the overall symmetry which is important.

Orientation of the Image Point and Symmetry

In this connection the influence of anisotropy of the image point to the symmetry is important. Figure 10 schematically shows as demonstrated on the sections in Fig. 9 that the image points of composite adjacent sections penetrate in a different way into a section. The reproduction by the twofold axis remains error-free, as long as the long axis of the image point is perpendicular to the symmetry axis. In the other cases distortions will occur with translations of the adjacent projected sections in the positive and negative direction of the tilt axis, respectively. For this reason not all symmetries can in general be detected with the same significance. For molecule S 168-1-II the orientation of the image point is favourable with respect to the twofold axis. If, however, other twofold axes exist in the plane of the central wall, distortions will occur with respect to this axis. To study the structure of the central wall an orientation parallel to the support would be ideal. In such a case not only all twofold axes inside the wall but also symmetry axis along the long axis of the molecule could be detected. Such an orientation has not occured in our work up to now. However, two-dimensional micrographs already indicated molecules near this orientation. The geometrical distortion could be reduced with conical tilting, which produces less anisotropic image points.

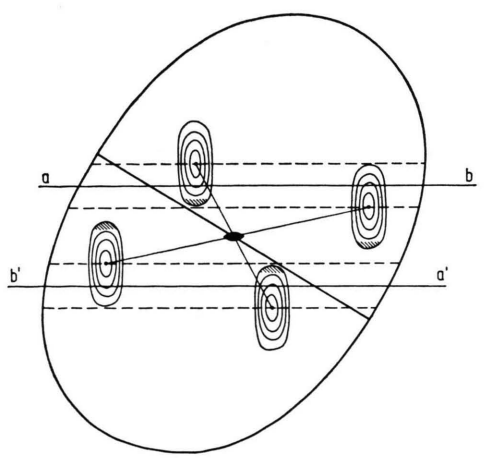

Fig. 10. Influence of anisotropic image points on the density in adjacent sections. With respect of the relative location of the image point and the density section, symmetry related sections are deformed differently.

The Structure of the Central Wall

The analysis of the molecule S-168-1-II has not only shown a twofold axis but has also demonstrated that this symmetry condition seemed to be best conserved in the regions near the central wall. Figure 8 proves that this wall is quite planar. Therefore, the structure of the central wall can be studied in a section through the wall. Such a study would also be important with respect to the symmetry around the long axis of the molecule according to the general conclusions of Fig. 4 and Figure 5. As the plane of the wall is parallel to the tilt axis according to Fig. 8, a rotation of 39° around this axis is necessary. It is evident that a study of the central wall in at least one further molecule would be of advantage. We have selected molecule S 168-1-I. Like all hitherto reconstructed molecules (except molecule S 168-1-II) it has a general orientation. In the first step the projection of long axis of the molecule onto the x, y-plane is rotated parallel to the x-axis. By studying the successive sections perpendicularly to the y-axis (like in Fig. 8) or by projecting the density along the y-axis (see Fig. 11, which corresponds to a virtual "micrograph" par-

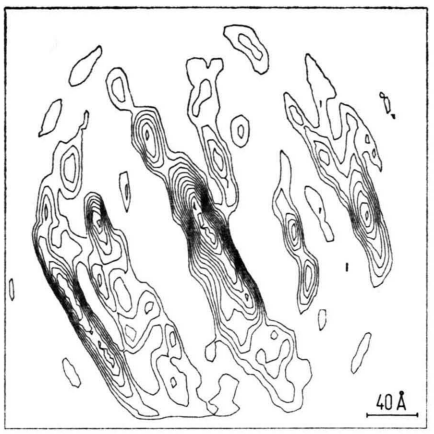

Fig. 11.

Fig. 11. Density-projection parallel to the central wall of molecule S 168-1-I and parallel to the surface of the supporting foil.

Fig. 12. Section through central wall of FAS-molecule S 168-1-II to find the position of the twofold axis.

Fig. 13. Section corresponding to Fig. 12 but for FAS-molecule S 168-1-I.

Fig. 14. Same as Fig. 12 with approximate sixfold symmetry of main density maxima. Pattern selection is optimal with this orientation. Detailed correlation studies should be performed.

Fig. 15. Same as Fig. 13 with fitting of density maxima present in Fig. 12 relating the features in the central walls of two different molecules.

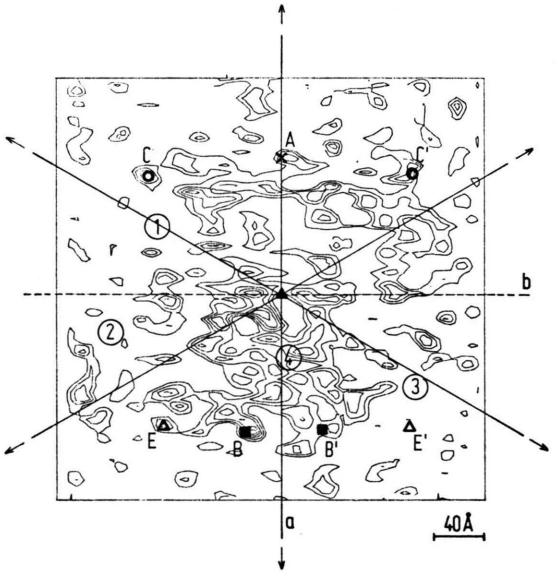

Fig. 12.

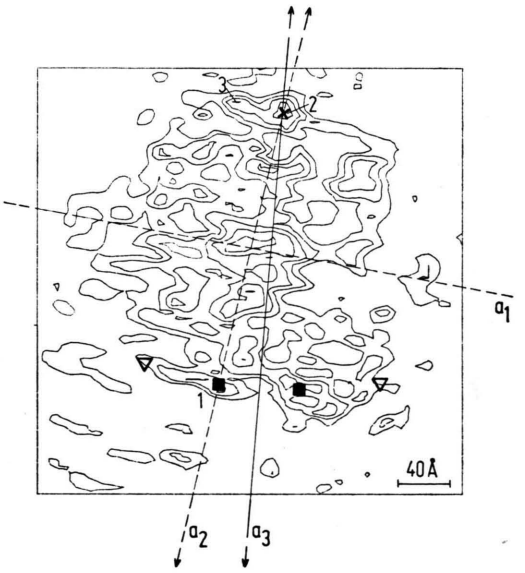

Fig. 13.

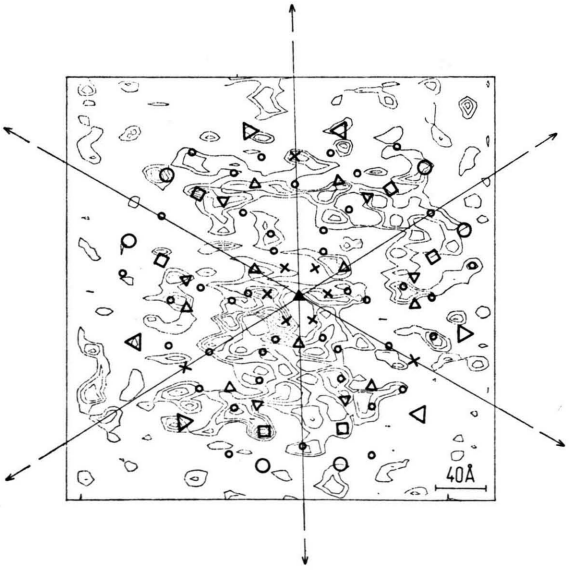

Fig. 14.

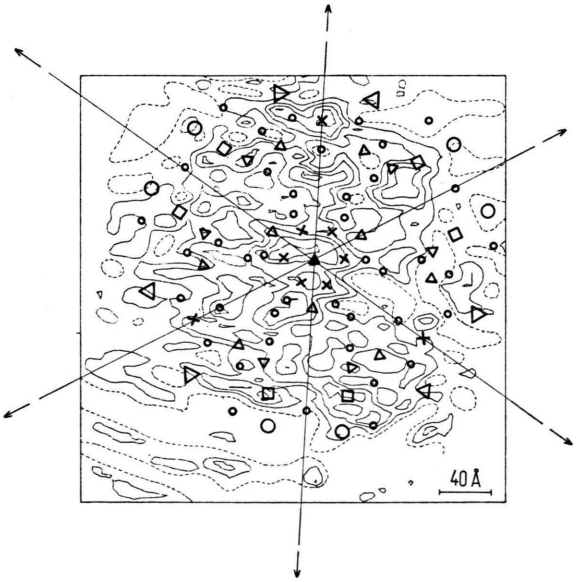

Fig. 15.

allel to the supporting foil!) the correct orientation of the wall and its planarity can be checked. In the second step the molecule will be rotated around the y-axis into the desired orientation with the central wall parallel to the x, y-plane. The rotation of the molecules with respect to both angles leads to difficulties, because the determination of the best orientation by few selected peaks might be in error due to a non-uniform stain distribution below and above the wall. Figure 12 and Fig. 13 show the central wall of the molecules S 168-1-II and S 168-1-I. Note the better resolution in Figure 12. The elongated image point in Fig. 12 will be cut at an angle of 40°. Therefore, the resolution is more isotropic than in Fig. 13 showing substantially elongated image points due to the small angle of 28° between the x, y-plane and the long axis of the image point.

The location of the section containing the twofold axis shown in Fig. 9 ($z = 33$ in Fig. 12, $z = 36$ in Fig. 13) will be determined by checking the twofold symmetry. This is done by comparison of the sections above and below the plane ($z = 35$ and $z = 37$ for molecule S 168-1-I, $z = 32$ and $z = 34$ for molecule S 168-1-II) in a similar way as described in Figure 9. Sections not containing the twofold axis should show additional distortions due to the inclined image point.

Let us first regard Figure 12. The twofold axis a (corresponding to the twofold axis in Fig. 9) can be recognized in spite of quite pronounced irregularities. The center of the wall – indicated by its intersection with the dashed line b – cannot be deduced from Fig. 12, as no symmetry with respect to this line is apparent. However, the center can be found approximately from the position of the outer wall of the ellipsoid in Figure 9. Figure 12 proves a quite detailed structure within the wall. For 6 asymmetric copies any additional symmetry would show point group symmetry 32 or 3 m. However, in contrast to the twofold symmetry discussed above such an additional symmetry is certainly not obvious. The overall stain distribution is not uniform. The regions ①, ②, ③ in Fig. 12 are especially strongly stained, the region ④ is only weakly stained. For the further analysis it turned out to be advantageous to select a few "guide peaks" (A, B, B′ in Figure 12). They should show no accidental mirror symmetry with respect to line b and at least one peak of the two peaks related by the twofold symmetry should be well pronounced. For comparison with further molecules it is useful, to indicate additional auxiliary peaks (C, C′ and E, E′ in Figure 12). The guide peaks and the auxiliary peaks will now be repeated on a separate sheet by the suspected 3 m symmetry. The 6-fold point configurations will be fitted with small positional changes of the points to the section. This process can be repeated for further peaks. A point configuration will be accepted, if most of the points are represented by peaks or positive regions. Figure 14 shows a point distribution developed in this way and fitted to the section in Figure 12. It is evident that this trial and error procedure cannot produce the structure entirely correct, because too many uncertainties are involved in judging the significance of densities. However, this point structure follows the image in Fig. 12 fairly well.

This type of analysis is related to a Markham averaging [12] utilizing in our case the 6-fold 3 m symmetry. However, the procedure described above allows us to work with selected structural features and to judge their sixfold repetition individually. Another advantage is an easier location of a rotation axis and the possibility to recognize a deviation from the circular symmetry. Deviations could be suscepted from Fig. 14 although no systematic analysis has been attempted. However, the overall circular symmetry seems to be retained surprisingly well.

Let us now discuss Figure 13. Again a non-uniform staining can be observed. At the first glance one gets the impression of an approximate twofold symmetry, roughly connecting the right and the left side of Figure 13. A mirror line connecting the lower and the upper part of Fig. 13 is less probable, although the horizontal stripes through peaks 1 and 2 could crudely be interpreted as mirror images with respect to mirror line a_1. A mirror line a_2 connecting the peaks 1 and 2 seems to be quite obvious. The next step is to orient the points of Fig. 14 with respect to the vertical (a_2) and horizontal (a_1) "mirror line" and to shift it along the lines until the best fit is obtained. The same procedures must be repeated with an orientation change of 180°. Both trials proved to be unsuccessful. However, an attempt to correlate both structures with the help of the guide peaks and the auxiliary peaks (see Fig. 12) gave interesting results. In accordance with the above mentioned trials it was again impossible to fit the guide-auxiliary peaks A – C (Fig.

12) using the "mirror lines" a_1, a_2 as reference lines. Therefore we searched for other symmetry relations trying to fit simultaneously the guide-auxiliary peaks. From all possible choices only the mirror line a_3 gave a satisfactory fit, which has been confirmed by the fit of the remaining points to the peaks in Fig. 14 (compare Figure 15). The accuracy is less than in Fig. 14 due to the lower resolution. This was an intuitive choice because the elongated peaks are oriented nearly perpendicular to line a_2 and thus biasing this choice. It is obvious that Markham averaging would be very difficult in this case, as neither the symmetry line nor the center of the wall was recognizable in advance. Moreover an additional lowering of resolution with these elongated peaks would occur.

Discussion and Conclusions

We have mentioned in part I, that there might be difficulties in assessing the significance of a result in individual three-dimensional microscopy – the deduction of structural details needs confirmation by similar studies on other specimens. It is obvious that the analysis of a molecule consisting of n identical subunits corresponds in principle to an analysis of n specimens in the case of a one-unit molecule. Additional advantages are identical preparation and radiation conditions. As shown in this paper, the internal symmetries of the complex must be used to make these comparisons. It is a fundamental advantage of individual imaging (with regard to the averaging methods in the analysis of periodic arrays) that the individual images can be compared for a study of the kind of distortions etc.

In the case of FAS-molecules, an easily recognizable similarity of the subunits is not apparent, proving the enormous influence of preparation and – perhaps – of initial radiation damage. This is not surprising. Every electron microscopist knows the danger of artefacts in discussing conventional negatively stained micrographs. Three-dimensional microscopy removes the ambiguities due to neglecting the third coordinate. But it demonstrates the presence of distortions and artefacts in an even more impressive way than in projections.

The symmetry relations discussed in our case – especially within the central wall – are by no means obvious. But it is difficult to believe that the presented structural relations are purely accidental.

How can we proceed in our future work? The first and obvious possibility is to enlarge the experimental basis by comparing several molecules. Work along these lines is in progress. As shown above a careful non-trivial analysis is necessary. However, visual inspection is time consuming and only feasible in two dimensions. Computerized three-dimensional pattern recognition may be used, based for example on the convolution molecule method, introduced into crystallography several years ago [13, 14].

The second possibility concerns the combination of electron microscopy with supplementary methods. It is, for example, evident that our symmetry considerations would be more straight forward if the number of copies was already known from biochemical work. Interesting applications might be found in immuno electron microscopy, which already plays an important role in conventional microscopy.

However, most progress can be expected from the development of the experimental methods. Apart from the more "optical" developments (e. g. conical tilting) progress in the preparation technique is most important. This will be facilitated by the fact that three-dimensional electron microscopy allows a detailed study of the dependence of artefacts on the preparation method. Conventional negative staining is a quite crude procedure. Surface tension will try to distort the molecule, cavities will be partly filled due to the evaporation of the solvent. Similarly as first shown in "protein crystallography in the electron microscope" [15], the replacement of the water in the cavities by a water-equivalent non-evaporating medium might be a useful technique. To discriminate between stain and protein it should at least partly consist of heavy atoms. Perhaps a frozen glass-like heavy atom salt solution could be used for this purpose.

However, even the best preparation procedures would only be of value, if the specimen is not severely damaged by radiation. Let us discuss the approximate lower limits of radiation loading in the case of individual negatively stained specimens. If we assume for example a resolution of ~ 20 Å at a dose of $2 \cdot 10^{-3}$ C/cm^2 the relative standard deviation σ of the primary beam within a resolution element is ~ 0.04. In micrographs of negatively stained FAS molecules the averaged contrast $\Delta I/I$ between stained and non-stained regions is of the

order of 0.2. The signal to noise ratio $Q = \Delta I/I\,\sigma$ would then be ~ 5. As discussed in part II, three-dimensional reconstructions with 36 exposures ($\Delta\alpha = 5^\circ$, $\alpha_{max} = \pm 90^\circ$) at $Q = 5$ show only small noise contributions. The corresponding integral dose is $7.2 \cdot 10^{-2}$ C/cm². If we restrict α_{max} to $\pm 45^\circ$ in practice the integral dose will be lowered to $3.6 \cdot 10^{-2}$ C/cm² and the resolution element will be elongated in the z-direction to > 40 Å (thus leading to approximately the same noise contribution). However, it can be assumed that reconstructions with $Q = 3$ ($\sim 1.8 \cdot 10^{-2}$ C/cm²) or even with $Q = 2$ ($0.9 \cdot 10^{-2}$ C/cm²) should show the general features of the structure. In the case of molecules with more than one subunit, averaging will further improve the electron statistical significance. For example an averaged FAS subunit in a reconstruction with $Q = 2$ will be imaged with a virtual $Q \approx 5$. As known from the previously mentioned TMV-work [1] (recently confirmed by three-dimensional TMV-reconstructions at 0.15 C/cm² and $8 \cdot 10^{-3}$ C/cm² [16]) the radiation damage influence, at doses of the order 10^{-2} C/cm² and at resolutions of ~ 20 Å, is certainly very low. Therefore, it is not improbable that preparation and radiation damage could be matched in future. However, it is evident that the development of an experimental technique of collecting three-dimensional data at extremely low doses, eliminating entirely pre-illumination, will be necessary.

The best experimental tool for low dose three-dimensional microscopy would be – as mentioned in part I – a three-dimensionally imaging microscope [17]. As reported elsewhere [18] even high resolution work on individual organic molecules utilizing redundancies in structural radiation chemistry might then be possible.

Supported by the Deutsche Forschungsgemeinschaft (the biological work especially by the Sonderforschungsbereich 51, Medizinische Molekularbiologie und Biochemie in München) and the Fonds der Chemischen Industrie. We should like to express our sincere thanks.

[1] R. C. Williams and H. W. Fisher, J. Mol. Biol. **52**, 121 [1970].
[2] M. Echert and W. Hoppe, in preparation. – The first electron micrographs of FAS have been reported by A. Hagen and P. Hofschneider, Third Europ. Reg. Conf. on Electr. Micr. 1964, Prague, Publishing House of the Czechoslovak Akademy of Sciences, pp. 69–70.
[3] W. Hoppe, Proc. Eighth Intern. Congr. on Electr. Micr., Canberra, Vol. **I**, p. 308 [1974].
[4] W. Hoppe, J. Gaßmann, N. Hunsmann, H. J. Schramm, and M. Sturm, Hoppe-Seyler's Z. Physiol. Chem. **355**, 1483 [1974].
[5] F. Lynen, Current Trends in the Biochemistry of Lipids, Ed. J. Ganguly and R. M. S. Smellie, Acad. Press London and New York 1972, p. 5–26.
[6] E. Schweizer, B. Kniep, H. Castorph, and U. Holzner, Eur. J. Biochem. **39**, 353 [1973].
[7] We thank Prof. Dr. F. Lynen and collaborators for supplying fatty acid synthetase.
[8] R. Langer, Ch. Poppe, H. J. Schramm, and W. Hoppe, J. Mol. Biol. **93**, 159 [1975].
[9] M. Müller and Th. Koller, Optik **35**, 287 [1972].
[10] Th. Koller, M. H. Hahn, and H. Waldner, Optik **35**, 319 [1972].
[11] I. Pilz, M. Herbst, O. Kratky, D. Oesterhelt, and F. Lynen, Eur. J. Biochem. **13**, 55 [1970]. – Also micrographs of freeze-etched and shadowed FAS indicate a body with a closed outer wall (private communication, D. Oesterhelt, W. Stoeckenius).
[12] R. Markham, S. Frey, and G. J. Hills, Virologie **20**, 88 [1963].
[13] W. Hoppe, Z. Elektrochem. **61**, 1076 [1957].
[14] R. Huber, Crystallographic Computing, Ed. F. R. Ahmed, Munksgaard Copenhagen 1970, p. 96–102.
[15] W. Hoppe, R. Langer, G. Knesch, and Ch. Poppe, Naturwiss. **55**, 333 [1968].
[16] W. Hoppe, H. Wenzl, and H. J. Schramm, Proc. Sixth Europ. Congr. on Electr. Micr. 1976, Jerusalem, Tal Int. Publ. Comp., Ed. D. G. Brandon, Vol. II, pp. 58–60. – W. Hoppe, H. Wenzel, and H. J. Schramm, Hoppe-Seyler's Z. physiol. Chem., submitted.
[17] W. Hoppe, Z. Naturforsch. **27 a**, 919 [1972].
[18] W. Hoppe, Z. Naturforsch. **30 a**, 1188 [1975].